FORSCHUNGSZENTRUM
ROSSENDORF e.V.

FZR

FZR 93 - 01
January 1993

Reprint of Report ZfK - 690 (November 1989)

DYN3D/M2 - a Code for Calculation of Reactivity Transients in Cores with Hexagonal Geometry

Herausgeber:

U. Grundmann und U. Rohde

Abstracts

The code DYN3D/M2 consists of the 3-dimensional neutron kinetic model of the code HEXDYN3D and the thermohydraulic model of the code FLOCAL. The neutron kinetics of DYN3D/M2 is calculated by using a nodal expansion method (NEM) for hexagonal geometry. The developed method solves the neutron diffusion equation for two energy groups. Stationary state and transient behaviour can be calculated. By help of the code PREPAR-EC parameterized neutron physical constants of given burnup distribution can be transferred from the MAGRU library to an input file of DYN3D/M2. The code FLOCAL consisting of a two-phase coolant flow model, a fuel rod model and a heat transfer regime map up to superheated steam is coupled with neutron kinetics by the neutron physical constants. One coolant channel per fuel assembly and additional hot channels are considered. The activities for code validation and the range of application are described.

DYN3D/M2 - EIN RECHENPROGRAMM FÜR REAKTIVITÄTSTRANSIENTEN IN SPALTZONEN MIT HEXAGONALER GEOMETRIE

Das Rechenprogramm DYN3D/M2 besteht aus dem 3-dimensionalen neutronenkinetischen Modell des Codes HEXDYN3D und dem thermohydraulischen Modell des Codes FLOCAL. Die Neutronenkinetik von DYN3D/M2 wird mit Hilfe einer nodalen Entwicklungsmethode (NEM) für hexagonale Geometrie berechnet. Die entwickelte Methode löst die Neutronendiffusionsgleichung für zwei Energiegruppen. Mit Hilfe des Codes PREPAR-EC werden parametrisierte neutronenphysikalische Konstanten für eine gegebene Abbrandverteilung aus der MAGRU-Bibliothek auf eine Eingabedatei von DYN3D/M2 geschrieben. Das Programm FLOCAL, das aus einem Zweiphasen-Strömungsmodell, einem Brennstabmodell und einer Wärmeübergangskarte bis überhitzten Dampf besteht, ist mit der Neutronenkinetik über die neutronenphysikalischen Konstanten gekoppelt. Ein Kühlkanal pro Brennstoffkassette und zusätzliche Heißkanäle werden betrachtet. Die Aktivitäten zur Programmverifikation und der Anwendungsbereich werden beschrieben.

DYN3D/M2 - ПРОГРАММА ДЛЯ РАСЧЕТА АВАРИЙ С РЕАКТИВНОСТЬЮ В АКТИВНЫХ ЗОНАХ С ГЕКСАГОНАЛЬНОЙ ГЕОМЕТРИЕЙ

Программа DYN3D/M2 состоит из трехмерной нейтронно-кинетической модели в виде программы HEXDYN3D и теплогидравлической модели программы FLOCAL. В нейтронно-кинетической части DYN3D/M2 используется узловой метод для гексагональной геометрии. С помощью разработанного метода решается уравнение диффузии нейтронов в двухгрупповом приближении. Можно рассчитать стационарное состояние и нестационарное поведение. Параметризованные физические константы для данного состояния выгорания могут быть переданы с помощью программы PREPAR-EC из библиотеки MAGRU в вводный файл программы DYN3D/M2. Программа FLOCAL включает моделирование двухфазного течения теплоносителя, поведения твэла и карту режимов теплопередачи вплоть до перегретого пара и связана с нейтронной кинетикой через нейтронно-физические константы. Рассматриваются средний теплогидравлический канал для каждого пакета твэлов и дополнительные горячие каналы. Описываются работы по аппробации кода и область применимости.

Content

1. Introduction

The model of the 3 - dimensional transient code DYN3D/M2 developed for thermal reactors with hexagonal geometry is described in this paper. The code can be used for calculations of reactivity initiated accidents (RIA) of VVER - type reactor cores.
If we consider moved control rods, a more detailed analysis of cores in comparison to point and one - dimensional kinetic models is possible by help of this code, describing the 3 - dimensional effects of power release. Furthermore, the influence of different changes of thermohydraulic properties in different assemblies on the reactivity feedback is taken into account. Reactivity changes induced by different changes of coolant inlet temperatures or boron concentrations of fuel assemblies can be investigated also. Several values being important for the safety margin as DNB - ratio, fuel enthalpy, cladding temperature and degree of oxidation are calculated. The transient processes in the core can be investigated as long as the core geometry is maintained.
The code consists of two parts: neutron kinetics and thermohydraulics, the connection of which is given by an parameterized dependence of the constants of diffusion equation from the thermohydraulic properties fuel temperatures, moderator temperatures, moderator densities and boron concentrations.
The 3 - dimensional neutron kinetics based on the solution of time dependent diffusion equations for two energy groups is treated by using a nodal expansion method (NEM) developed firstly for stationary problems /1/ and extended to time dependent problems. The methods solving stationary and transient problem and the dependence of neutron group constants are described in Chapter 2.
The thermohydraulic model of the core (code FLOCAL) is based on a two phase flow model for flow regimes up to superheated vapour. A simple model describing the fuel rod behaviour under transient conditions is included in FLOCAL. A simple cross flow model is under testing. The fundamental approximations of equations and mathematical methods of FLOCAL are given in Chapter 3.
Some work for the validation of both parts neutron kinetics and thermohydraulics was carried out. Benchmark solutions and comparisons with other codes are used for stationary problems. Reactivity measurements and kinetic experiments at the zero power reactor LR-0 were compared with the calculated results (Chapter 4). the validation activties of FLOCAL are described in Chapter 5. These activities involve validation of separate effect models, comparison with similar codes and benchmark solutions, calculations to RIA experiments from literature and some sensitivity studies. Some remarks to the range of application are given in Chapter 6.

2. Neutron Flux Calculation

2.1. Stationary Case

The 3-dimensional neutron distribution is calculated by solving the diffusion equation for two energy groups with help of a nodal expansion method for hexagonal geometry, used firstly in the stationary code HEXNOD23 /1/.
If the core consisting of hexagonal fuel assemblies is divided into a given number of slices, the nodes are the parts of the fuel assemblies in each slice. The neutron group constants are assumed to be spatially constant in each node n. The stationary diffusion equation can be written in the following form

$$\nabla\vec{J}_1^n(\vec{r}) + \Sigma_r^n \cdot \varphi_1^n(\vec{r}) = \frac{1}{k_{eff}} \sum_{g=1}^{2} \nu\Sigma_{fg}^n \cdot \varphi_g^n(\vec{r})$$

$$\nabla\vec{J}_2^n(\vec{r}) + \Sigma_a^n \cdot \varphi_2^n(\vec{r}) = \Sigma_s^n \cdot \varphi_1^n(\vec{r}) \qquad (2.1)$$

with

φ_g^n - neutron fluxes of group g

$\Sigma_r^n, \Sigma_a^n, \Sigma_s^n$ - macroscopic removal, absorption and transfer cross sections

ν_{fg}^n - macroscopic fission cross sections of group g multiplied by the number of fission neutrons

in the node n and

k_{eff} - stationary eigenvalue

Using Fick's law and the diffusion coefficients D_g^n we obtain the relation between the currents J_g and φ_g

$$\vec{J}_g^n = - D_g^n \cdot \nabla\varphi_g^n(\vec{r}) \qquad (2.2)$$

Integration of Eq. (2.1) over the node volume V^n yields the nodal balance equations

$$\sum_m \frac{F^{n,m}}{V^n} J_1^{n,m} + \Sigma_r^n \cdot \Phi_1^n = \frac{1}{k_{eff}} \cdot \sum_{g=1}^{2} \nu\Sigma_{fg}^n \cdot \Phi_g^n$$

$$\sum_m \frac{F^{n,m}}{V^n} J_2^{n,m} + \Sigma_a^n \cdot \Phi_2^n = \Sigma_s^n \cdot \Phi_1^n \qquad (2.3)$$

with
$F^{n,m}$ - interface between node n and neighbouring node m
Φ_g^n - mean neutron flux of group g in the node n
$J_g^{n,m}$ - mean net current of group g at the interface $F^{n,m}$

Now the partial currents $j_g^{n,m}$ (outgoing) and $j_g^{m,n}$ (incoming) are introduced by

$$j_g^{n,m} = 1/2\ (1/2\ \Phi_g^{n,m} + J_g^{n,m})$$
$$j_g^{m,n} = 1/2\ (1/2\ \Phi_g^{n,m} - J_g^{n,m}) \qquad (2.4)$$

with the mean fluxes $\Phi_g^{n,m}$ at the interface $F^{n,m}$.
The interface conditions of diffusion theory are fulfilled in a integral sense, i. e. at the interfaces continuity of mean fluxes and net currents or continuity of mean partial currents in both directions are required.
If n is a node at the system boundary and m stands for the outer space, the following conditions are taken into account

$$j_1^{m,n} = \tilde{R}_{11} \cdot j_1^{n,m}$$
$$j_2^{m,n} = \tilde{R}_{21} \cdot j_1^{n,m} + \tilde{R}_{22} \cdot j_2^{n,m} \qquad (2.5)$$

with given albedo coefficients $\tilde{R}_{gg'}$.
Using the integral balance Eqs. (2.3) for solving the problem, we need additional relations between mean fluxes Φ_g^n and partial currents $j_g^{n,m}$, $j_g^{m,n}$, obtained by a approximate solution of diffusion equation in the nodes. Considering in the following any node n, we will omit the index n of the node. The partial currents at the six radial surfaces of the hexagonal prism are signed by $j_{g,i}^{out}$, $j_{g,i}^{in}$ (Fig. 1). $j_{g,u}^{out}$, $j_{g,u}^{in}$ and $j_{g,l}^{out}$, $j_{g,l}^{in}$ are the partial currents at the upper and lower surface respectively.
In the applied method the space dependence of fluxes inside the nodes is separated in the axial direction and the hexagonal plane

$$\varphi_g(\vec{r}) = \Phi_g \cdot \psi_g(x,y) \cdot f_g(z) \qquad (2.6)$$

Using for $\psi_g(x,y)$ an expansion with Bessel functions and for $f_g(z)$ an expansion up to the fourth order, we obtain the

following relations between mean fluxes and mean partial currents (see Appendix A)

$$j^{out}_{g,i} = \sum_{g'=1}^{2} P_{g,g'} \cdot \Phi_{g'} + \sum_{i'=1}^{6} \sum_{g'=1}^{2} W^{i,i'}_{g,g'} \cdot j^{in}_{g',i'} \qquad (2.7)$$

and

$$\begin{aligned} j^{out}_{g,u} &= \alpha_g \cdot (\Phi_g + C_{4,g}) - a_g \cdot j^{in}_{g,u} - b_g \cdot j^{in}_{g,l} + \eta_g \cdot C_{3,g} \\ j^{out}_{g,l} &= \alpha_g \cdot (\Phi_g + C_{4,g}) - b_g \cdot j^{in}_{g,u} - a_g \cdot j^{in}_{g,l} - \eta_g \cdot C_{3,g} \end{aligned} \qquad (2.8)$$

The coefficients and the equations for the coefficients $C_{3,g}$ and $C_{4,g}$ of the higher polynomials are described also in App. A. By means of these relations, the integral balance equations (2.3) and the boundary conditions (2.5) the 3-dimensional problem can be solved. The numerical problem is treated by an iteration process consisting of inner and outer iteration cycles. Fission source iteration with Chebyshev acceleration technique is applied for the outer cycle. Due to the good convergence only few inner iterations (1 - 3 cycles) are necessary to reach a sufficient accuracy. During the iteration process recalculations of the matrix elements in Eq. (2.7) are necessary, but only few (4 - 5 times) recalculations are sufficient by the weak dependency of the elements from the transversal bucklings and k_{eff}.
Non-multiplying nodes as reflector or absorber can be described either by boundary conditions or by artificial assemblies with equivalent diffusion constants.

2.2. Time Dependent Case

Calculating transient processes, we must solve the time dependent neutron diffusion equation including the equations for delayed neutrons for all nodes n

$$\frac{\partial\varphi_1^n(\vec{r},t)}{v_1^n\partial t} + \nabla\vec{J}_1^n(\vec{r},t) + \Sigma_r^n(t)\cdot\varphi_1^n(\vec{r},t) = \frac{1}{k_{eff}}\sum_{g=1}^{2}(1-\beta_g^n)\nu\Sigma_{fg}^n\cdot\varphi_g^n(\vec{r},t) + \sum_{j=1}^{M}\lambda_j\cdot c_j^n(\vec{r},t)$$

(2.9)

$$\frac{\partial\varphi_2^n(\vec{r},t)}{v_2^n\partial t} + \nabla\vec{J}_2^n(\vec{r},t) + \Sigma_a^n(t)\cdot\varphi_2^n(\vec{r},t) = \Sigma_s^n(t)\cdot\varphi_1^n(\vec{r},t)$$

$$\frac{\partial c_j^n(\vec{r},t)}{\partial t} = \frac{1}{k_{eff}}\sum_{g=1}^{2}(1-\beta_g^n)\nu\Sigma_{fg}^n\cdot\varphi_g^n(\vec{r},t) - \lambda_j\cdot c_j^n(\vec{r},t)$$

$$j = 1,2,.....,M$$

(2.10)

$$\beta_g^n = \sum_{j=1}^{M}\beta_{g,j}^n$$

$$g = 1,2$$

where

v_g^n - mean group velocities of neutrons

$c_j^n(\vec{r},t)$ - density of precursors of typ j

$\beta_{g,j}^n$ - effective fractions of delayed neutrons of group j for a fission with an incident neutron of group g in the node n and

M - number of different precursor groups

λ_j - decay constant for precursors of group j

One set of decay constants is used for the whole core, because the decay constants of precursors arising from different fissionable isotopes are not much different. In thermal reactors the main part of prompt and delayed neutrons comes from fissions by

thermal neutrons. Therefore at the beginning of fuel cycle a sufficient accuracy of time behaviour is reached by using only one set of $\beta^n_{g,j}$, which are the effective constants of the considered core.

Methods published in /2/ are applied for solving the time dependent equations. Integrating over the node volume V^n we obtain the time dependent balance equations of the nodes

$$\frac{d\Phi^n_1(t)}{v^n_1 \cdot dt} + \sum_m \frac{F^{n,m}}{V^n} J^{n,m}_1(t) + \Sigma^n_r(t) \cdot \Phi^n_1(t) = \frac{1}{k_{eff}} \sum_{g=1}^{2} (1-\beta^n_g) \nu\Sigma^n_{fg}(t) \cdot \Phi^n_g(t) + \sum_{j=1}^{M} \lambda_j \cdot C^n_j(t)$$

$$\frac{d\Phi^n_2(t)}{v^n_2 \cdot dt} + \sum_m \frac{F^{n,m}}{V^n} J^{n,m}_2(t) + \Sigma^n_a(t) \cdot \Phi^n_2(t) = \Sigma^n_s(t) \cdot \Phi^n_1(t) \qquad (2.11)$$

with

$$\frac{dC^n_j(t)}{dt} = \frac{1}{k_{eff}} \sum_{g=1}^{2} \beta^n_{g,j} \nu\Sigma^n_{fg}(t) \cdot \Phi^n_g(t) - \lambda_j \cdot C^n_j(t) \qquad (2.12)$$

$$j=1,2,\ldots,M$$

$C^n_j(t)$ - mean value of precursor density $c^n_j(\vec{r},t)$

An exponential transformation technique known for example from /2/ is used for the time integration of Eqs (2.11). We define

$$\Phi^n_g(t') = \exp[\Omega^n(t'-t+\Delta t)] \cdot \tilde{\Phi}^n_g(t') \qquad (2.13)$$

for

$$t - \Delta t \leq t' \leq t$$

Using an implicite difference scheme we replace the time derivative of neutron fluxes in Eq. (2.11) by

$$\frac{d\Phi^n_g(t)}{dt} \approx 1/\Delta t \cdot [(1 + \Omega^n \Delta t) \cdot \Phi^n_g(t) - \exp(\Omega^n \cdot \Delta t) \cdot \Phi^n_g(t - \Delta t)] \qquad (2.14)$$

Ω^n is given from the previous time step or can also determined during the iteration process.

$$\Omega^n = 1/\Delta t \cdot \ln[\sum_{g=1}^{2} \Phi_g^n(t) / \sum_{g=1}^{2} \Phi_g^n(t-\Delta t)] \qquad (2.15)$$

Assuming an exponential behaviour for $\Phi_g^n(t)$ and $\nu\Sigma_{fg}^n$ constant in the interval Δt, we can approximately integrate the equations of precursors

$$C_j^n(t) = C_j^n(t-\Delta t) \cdot \exp(-\lambda_j \cdot \Delta t) \qquad (2.16)$$

$$+ \frac{1-\exp[-(\lambda_j+\Omega^n)\Delta t]}{(\Omega^n + \lambda_j)} \cdot \frac{1}{k_{eff}} \sum_{g=1}^{2} \beta_{g,j} \nu\Sigma_{fg}^n(t) \cdot \Phi_g^n(t)$$

Inserting Eq. (2.14) together with (2.16) in Eqs. (2.11) we obtain an inhomogeneous stationary equation system for $\Phi_g^n(t)$. It can be solved with help of relations between partial currents and mean fluxes. Deriving these relations for the time dependent problem, some approximations are applied. Thus we made the assumption, that in Eq. (2.9) the source of delayed neutrons is proportional to the prompt fission source /2/:

$$c_j^n(\vec{r},t) = \frac{\sum_{g=1}^{2} \beta_{g,j}^n \nu\Sigma_{fg}^n(t) \cdot \varphi_g^n(\vec{r},t)}{\sum_{g=1}^{2} \beta_{g,j}^n \nu\Sigma_{fg}^n(t) \cdot \Phi_g^n(t)} \cdot C_j^n(t) \qquad (2.17)$$

and the time derivative is calculated approximately by assuming an exponential behaviour with the Ω^n of the previous time step

$$\frac{\partial \varphi_g^n(\vec{r},t)}{v_g^n \cdot \partial t} \approx \frac{\Omega^n}{v_g^n} \cdot \varphi_g^n(\vec{r},t) \qquad (2.18)$$

With these assumptions, Eqs. (2.9) are transformed in homogeneous equations, which can be treated similar to the stationary case (Appendix A) and analogous Eqs. (A12) - (A18) and (A23) - (A27)

are obtained. In the code the matrices of Eqs. (A12) are determined at the begin of each time step iteration. Similar to the stationary case the time step iteration is split in inner and outer iteration cycles. The outer iteration differs from the homogeneous case by the additional fixed source of Eqs. (2.11). Chebyshev scheme is also used for acceleration of outer iterations.
Before using this method in the code DYN3D/M2 the neutron kinetics code HEXDYN3D and the dynamic code DYN3D/M1 including a simple thermohydraulic model was developed.

2.3. Neutron Physical Constants

Applying a parameterized or tabular form for the dependence of neutron group constants from the thermal quantities fuel temperature T_F^n, moderator temperature T_M^n, moderator density ϱ_M^n and the mass specific boron acid concentration c_B^n of each node n one can calculate the constants of actual thermohydraulic variables. The parameterized dependence used in DYN3D/M2 is based on the results of the code PREPAR-EC and has for any cross section Σ of (2.1) or the diffusion coefficients D the following form:

$$\begin{aligned}\Sigma^n = \Sigma_o^n \cdot \{1 + \tilde{\alpha}_\Sigma^n \cdot [(T_M^n)^{-1/2} - (T_{M,o})^{-1/2}]\} \\ \cdot \{1 + \tilde{\beta}_{\Sigma,1}^n \cdot (\varrho_M^n - \varrho_{M,o}) + \tilde{\beta}_{\Sigma,2}^n \cdot (\varrho_M^n - \varrho_{M,o})^2\} \\ \cdot \exp\{\tilde{\gamma}_\Sigma^n \cdot [(T_F^n)^{1/2} - (T_M^n)^{1/2}]\} \\ \cdot \{1 + \tilde{\delta}_{\Sigma,1}^n \cdot (c_B^n \varrho_M^n - c_{B,o}\varrho_{M,o}) + \tilde{\delta}_{\Sigma,2}^n \cdot (c_B^n \varrho_M^n - c_{M,o}\varrho_{M,o})^2\}\end{aligned} \qquad (2.19)$$

with reference values Σ_o^n, $T_{M,o}$, $\varrho_{M,o}$ and $c_{M,o}$. By help of the code PREPAR-EC an input file with the needed constants $\{T_{M,o}$, $\varrho_{M,o}$, $c_{B,o}$, Σ_o^n, $\tilde{\alpha}_\Sigma^n$, $\tilde{\beta}_{\Sigma,1}^n$, $\tilde{\beta}_{\Sigma,2}^n$, $\tilde{\gamma}_\Sigma^n$, $\tilde{\delta}_{\Sigma,1}^n$ and $\tilde{\delta}_{\Sigma,2}^n\}$ of a given burnup distribution can be generated from the MAGRU-EC library/3/.
Calculating the stationary state an iteration between neutron flux and thermohydraulic calculation is carried out until a given accuracy of the distribution is reached. The eigenvalue k_{eff} or the boron concentration can be determined for a given power. The time behaviour of the group constants is given by changes of thermohydraulic properties for describing feedback or explicitly by alteration of the typ in the case of moved control rod. Regarding a time step Δt, the thermohydraulic properties of the last step are used for calculation of neutron kinetics. An iteration between both parts of code is also possible.

3. FLOCAL - the Model for Core Thermohydraulic Analysis

3.1. Characteristics of the FLOCAL Model

The model for the evaluation of core thermohydraulics during reactivity-initiated transients is based on following principles:

A The core is represented by one-dimensional parallel coolant channels . Each coolant channel is connected to a fuel assembly. The channels can be considered as isolated (no cross flow is taken into account) or a simple approximation for the evaluation of cross flow between the channels can be used. Furthermore , fictive hot channels can be considered for analyzing the effect of power peaks , coolant temperature , flow rate or fuel parameters uncertainties.

B The flow model (one- and two-phase flow) is based on four differential balance equations for mass , energy and momentum of the mixture and mass balance of the vapour phase. In this way a dynamical description of thermal non-equilibrium effects is possible. The phase slip is taken into account in quasi-static manner by a slip correlation.

C The thermohydraulic model is closed by constitutive laws for one- and two-phase frictional pressure drops , evaporation and condensation rate , heat transfer coefficients and thermophysical properties of the phases.

D For the fuel rod the one-dimensional heat conduction equation is solved.

In the following the set of equations is listed:

-momentum balance of the mixture

$$\partial/\partial t[\varphi\varrho_v u_v+(1-\varphi)\varrho_l u_l] + \partial/\partial z[\varphi\varrho_v u_v^2+(1-\varphi)\varrho_l u_l^2]$$

$$+ \partial p_{fric}/\partial z + g[\varphi\varrho_v+(1-\varphi)\varrho_l] + \partial p/\partial z = 0 \qquad (3.1)$$

-energy balance of the mixture

$$\partial/\partial t[\varphi\varrho_v h_v+(1-\varphi)\varrho_l h_l] + \partial/\partial z[\varphi\varrho_v u_v h_v+(1-\varphi)\varrho_l u_l h_l] = Q \qquad (3.2)$$

$$Q = \alpha(T_W - T_l)A/V$$

-mass balance of the mixture

$$\partial/\partial t[\varphi\varrho_v+(1-\varphi)\varrho_l] + \partial/\partial z[\varphi\varrho_v u_v+(1-\varphi)\varrho_l u_l] = 0 \qquad (3.3)$$

-mass balance of the vapour phase

$$\partial/\partial t(\varphi\varrho_v) + \partial/\partial z(\varphi\varrho_v u_v) = \mu \qquad (3.4)$$

-heat conduction equation

$$\varrho c\partial T/\partial t = 1/r\cdot\partial/\partial r(\lambda r\cdot\partial T/\partial r) + q \qquad (3.5)$$

for cladding or fuel , q - heat source density,

-equations of state for the phases

$$\varrho_v = f_v(h_v,p) \qquad T_v = F_v(h_v,p)$$
$$\varrho_l = f_l(h_l,p) \qquad T_l = F_l(h_l,p) \qquad (3.6)$$

-constitutive laws for frictional pressure drop $\partial p_{fric}/\partial z$, evaporation and condensation rate μ , slip ratio $s=u_v/u_l$ and heat transfer coefficient α from wall to coolant.
h is the enthalpy , ϱ the density , u the velocity of vapour (v) or liquid (l) phase , φ is the void fraction and p the pressure . Introducing following two-phase mixture parameters

$$h = xh_v + (1-x)h_l \qquad \text{mixture enthalpy}$$
$$G = \varphi\varrho u_v + (1-\varphi)\varrho_l u_l \qquad \text{mass velocity}$$
$$\varrho = \varphi\varrho_v + (1-\varphi)\varrho_l \qquad \text{mixture density} \qquad (3.7)$$
$$\varrho^* = \partial\varphi/\partial x\cdot[x\varrho_l+(1-x)\varrho_v] \qquad \text{vapour mass transport density}$$
$$v_I = x^2/\varphi\varrho_v + (1-x)^2/(1-\varphi)\varrho_l \qquad \text{inverse density for momentum transport}$$

and taking into account the relation between flowing quality x and void fraction φ

$$\varphi = \frac{1}{1 + (1-x)\varrho_v s/x\varrho_l}$$

the equations (3.1) to (3.4) can be transformed into the conser-

vative form:

$$\partial G/\partial t + \partial/\partial z(G^2 v_I) + \partial p_{fric}/\partial z + g\varrho + \partial p/\partial z = 0 \qquad (3.8)$$

$$\varrho\partial h/\partial t + G\partial h/\partial z = Q + \partial X/\partial t \qquad (3.9)$$

$$\partial\varrho/\partial t + \partial G/\partial z = 0 \qquad (3.10)$$

$$\varrho^* \partial\varphi/\partial t + G\partial x/\partial\varphi \cdot \partial\varphi/\partial z = \mu + \partial x/\partial p \cdot [\varrho^* \partial\varphi/\partial x \cdot \partial p/\partial t + G\partial p/\partial z) \qquad (3.11)$$

with $X = (h_V - h_l)[(1-\varphi)x\varrho_l - \varphi(1-x)\varrho_V]$

Additionally , a balance equation for soluble poisson (boron acid concentration) is considered:

$$\varrho\partial c_B/\partial t + G\partial c_B/\partial z = 0 \qquad (3.12)$$

c_B is the mass specific boron acid concentration in g/kg.
In this representation the two-phase flow equations correspond to the balance equations for a homogeneous or one-phase flow. In this way numerical methods for one-phase flow equations can be applied. The inhomogeneity of the flow is taken into account by the definition of effective two-phase flow parameters (3.7) what leads to different effective velocities for mass , momentum and energy transport and the additional source term $\partial X/\partial t$ in the energy equation.

E Boundary conditions for the core (coolant inlet temperature , pressure , pressure drop over the core or mass flow rate and boron acid concentration at the inlet) determined by the coolant loops behaviour , must be given as functions of time in form of a table. Thermal power is taken from the 3D kinetics.
For coolant inlet temperature and boron acid concentration a profile over the assemblies can be given. A lower plenum mixing model for the determination of this inlet profile from the parameters of the primary circuit loops based on experimental investigations for VVER-440 type reactors is under preparation.
The boundary conditions for coolant flow can be given in following options:
- flow rate for each assembly,
- pressure drop over the core (iterative estimation of assembly flow rates with the condition of equal pressure drop),
- total mass flow rate through the core (iterative determination of flow rate distribution with the condition of equal pressure drop).

F A simple cross flow model based on the assumption , that no radial pressure gradients occur , is available. In the frame of this model mass flow rates in each axial node of each assembly are determined by the conditions of equal pressure drop over all nodes in the plane and given total mass flow rate m_{tot}:

$$\Delta p_{i,1} = \Delta p_{i,2} = \ldots = \Delta p_{i,k}$$

$$\sum_k m_{i,k} = m_{i,tot} \qquad (3.13)$$

i - index of axial plane , k - index of coolant channel (assembly).
Under steady-state conditions m_{tot} is equal for all axial positions , in transient processes the integral mass balance equation has to be taken into account:

$$m_{i+1,tot} = m_{i,tot} - \sum_k A_k \int_{z_i}^{z_{i+1}} \partial \varrho_k / \partial t \, dz \qquad (3.14)$$

In this way the mass flow rate redistribution is evaluated , but the energy and momentum transfer by cross flow is not taken into account (the balance equations are solved without exchange terms). Turbulent mixing is also neglected.
The method allows a very fast estimaton of cross flow effects assuming the cross flow resistance coefficients to be zero , while in the approximation of isolated channels they are assumed to be infinite.

3.2. Constitutive Equations in the Thermohydraulic Model

Single pressure drops can be located at the inlet and the outlet of coolant channels and at spacer grids positions. They are described by resistance coefficients ζ.
The two-phase multiplier for single pressure losses is estimated by the homogeneous model:

$$\Delta p_{single} = \zeta \cdot \frac{G^2}{2\varrho_l} \cdot \Phi_{hom} \;, \quad \Phi_{hom} = 1 + x(\varrho_l/\varrho_v - 1) \qquad (3.15)$$

The friction coefficient for the fuel rod bundle is evaluated by a correlation of FILONENKO with a bundle correction , the two-phase multiplier for the frictional pressure drop is determined by a correlation of OSMACKIN ,following literature recommendations /4/.
μ in equation (3.11) describes the evaporation rate by heat

supply and condensation rate in subcooled liquid. Adiabatic evaporation due to pressure change is taken into account by the second source term in equ. (3.11). For μ a modification of the subcooled boiling model by MOLOCNIKOV /5/ is used:

$$\mu_{evap} = xq''/r \ , \ x = \begin{cases} \tanh\left(3{,}5\,\dfrac{h_l - h_{BO}}{\Delta h_{BO}}\right) & \text{for } h_l > h_{BO} \\ 0 & \text{for } h_l < h_{BO} \end{cases} \qquad (3.16)$$

q" is the thermal power density in the coolant , r is the evaporation heat , h_{BO} the liquid enthalpy at boiling onset, $\Delta h_{BO} = h_{sat} - h_{BO}$.
The onset of subcooled boiling is assumed , when the cladding surface temperature approaches the transition point from convective to boiling heat transfer , determined by the used heat transfer correlations. The condensation rate in subcooled liquid is described by the expression :

$$\mu_{cond} = C \cdot F(G) \frac{(h_l - h_{sat})}{r} \cdot \varphi \cdot [1+5\exp(-20\varphi)] \ , \ C=-17 m^{-1}$$

$$F(G) = \max \{f(g) \ , \ 400\} \quad \text{in } kg/(m^2 s) \ ,$$

$$f(G) = \begin{cases} G & \text{if } 3 < p < 10 \text{ MPa}, \\ 400\ (G/400)^{p/3} & \text{if } p < 3 \text{ MPa}, \\ 2000\ (G/2000)^{p/10} & \text{if } p > 10 \text{ MPA} \end{cases} \qquad (3.17)$$

Here a modification of the original model is made (in the original model F(G) = G) , what improves the results in comparison with experiments , especially at low and high pressure values (see section 5).
For the calculation of the phase slip ratio the corresponding to the MOLOCNIKOV model slip correlation is used :

$$s = u_v/u_l = 1+(0{,}6+1{,}5\beta)/Fr^{0.25} \cdot (1-p/p_{crit})[1-\exp(-20\beta)]^{1/2} \qquad (3.18)$$

$$\beta = \left[\ 1 + \frac{(1-x)\varrho_v}{x\varrho_l}\ \right]^{-1} \ , \ Fr \text{ is the Froude number.}$$

An important role in the reactivity transient analysis plays the heat tranfer from fuel to coolant. It affects , on the one hand , the fuel temperature , being an important safety parameter , and influences the neutron kinetics behaviour via Doppler effect. On

the other hand , heat transfer crisis can occur at the cladding surface leading to wall superheating , what can result in cladding destruction.
The wall-to-coolant heat transfer model in FLOCAL is based on the heat transfer logic given by Fig. 3. In the pre-crisis region standard correlations from literature for one-phase liquid convection , boiling heat transfer and convective heat transfer in annular flow (regimes 1-3) are used /4/. The occurence of boiling crisis in low and high quality region is established by several correlations (OKB -2 /6/,IAE - 4 /7/ or BIASI /8/ for burnout , DOROSHCHUK - NIGMATULIN /9/ for dryout).
In /7/ a dynamical correction of the critical heat flux for transient processes is proposed introducing the retardation effect in heat flux integrals , which occur in the CHF - correlations :

$$\psi(z) = \int_0^z q''(z',t - \frac{z - z'}{w})\lambda e^{-\lambda(z-z')}/q''(z,t)\, dz'$$

$$H(z) = \int_0^z q''(z',t - \frac{z - z'}{w})/q''(z',t)\, dz' \qquad (3.19)$$

To avoid the relative expensive numerical calculation of the retarded heat flux integrals , an analytical estimation of the retardation effect is made , assuming an exponential change of heat flux in time with constant spatial shape. This dynamical correction can be applied to the BIASI - and IAE-4 correlations.
The transition boiling region (regime 4) is described by the KIRCHNER and GRIFFITH interpolation for the heat flux q" /10/:

$$q'' = q''_{crit}(T_w/T_{crit})^{\gamma}\ ,\ \gamma = \frac{\ln(q''_{crit}/q''_{MSFB})}{\ln(T_{crit}/T_{MSFB})} \qquad (3.20)$$

q''_{crit} is the critical heat flux.
The minimum stable film boiling point (Leidenfrost - temperature T_{MFSB}) is determined by a correlation based on experimental results from literature /11/:

$$T_{MSFB} = T_{sat} + 100 + 8(T_{sat} - T_l) \qquad (3.21)$$

In the stable post-crisis region (inverted annular flow or dispersed flow , regimes 5/6) the heat transfer coefficient is determined as the maximum of the MIROPOLSKIJ and modified BROMLEY correlation .

The effect of subcooling due to thermal non-equilibrium is taken into account by following correction factor to the post-crisis heat transfer coefficient:

$$\alpha_{pc} = \alpha_{pc}(T_l=T_{sat})\cdot(2T_{sat}/T_l - 1)^{1,5} \qquad (3.22)$$

After full evaporation of coolant , heat transfer to superheated steam is estimated by a forced convection correlation (regime 7).

The described heat transfer model allows the extension of thermo-hydraulic calculations beyond the DNB-limit and the estimation of wall temperatures in the post-crisis region.

3.3. Fuel Rod Model

For the evaluation of fuel and cladding temperatures the one-dimensional heat conduction equation in cylindrical geometry (3.5) is solved.
Thermal conductivity of fuel λ_f and cladding λ_{cl} can be constant or depending from temperature.
Gas gap between fuel and cladding plays an important role in the heat transfer behaviour. By this reason a simple deterministic gas gap model for short-time processes was implemented and can be used as an option. In the frame of this model the heat transfer components by conduction through the filling gas , radiation and conduction in the case of fuel-cladding contact are taken into account.The modeling of this heat transfer components is similar as in typical fuel rod behaviour codes (GAPCON-THERMAL ,SSYST).
The input information for the gas gap conductance model (cold gap width and gas pressure , gas composition) has to be got from detailed fuel rod analysis codes like STOFFEL /12/.
The model for the gap behaviour involves a simple modeling of cladding mechanics in membrane approximation including
-the determination of thermal and elastic deformations,
-the estimation of plastic deformations of the cladding , when the stress exceeds the yield point.
Plastic deformation can significantly influence the heat transfer behaviour in the high temperature region. In the typical for reactivity accidents situation when the outer pressure (coolant pressure) exceeds the inner gas pressure , plastic deformation leads to the closure of the gap and to intensification of heat transfer to the coolant.
Further , the metal-water reaction in high temperature region is considered. The additional heat source from this reaction is taken into account and the oxide layer thickness D is estimated

on the basis of the equation:

$$D \cdot dD/dt = A/C^2 \cdot \exp(-B/T) \qquad (3.23)$$

where T is the wall surface temperature and A,B,C are constants. The evaluation of cladding temperature , cladding stress and degree of cladding oxidation together with fuel enthalpy value at each axial position of the rod gives the possibility of fuel rod failure estimation.

3.4 Numerical Methods and Iterative Procedures in FLOCAL

In the following a brief characteristic of the numerical methods for solving the basic equations of the thermohydraulic model will be given.
The equations for energy balance (3.9) , vapour mass balance (3.11) and soluble poisson (3.12) are given in the conservative form :

$$\partial y/\partial t + u\partial y/\partial z = q$$

That's why the method of characteristics with linear interpolation between the mesh points can be used :

$$y_{i+1}^{n+1} = (1-c)y_{i+1}^{n} + cy_i^n + \Delta t/2(q_i^{n+1}+q_i^n) \qquad \text{if } c \leq 1$$

$$y_{i+1}^{n+1} = (1-c)/c \cdot y_i^{n+1} + 1/c \cdot y_i^n + \Delta t/2c[(2c-1)/c \cdot q_i^{n+1}+1/c \cdot q_i^n)$$

$$\text{if } c > 1 \qquad (3.24)$$

c is here the Courant parameter $c = u\Delta t/\Delta z$, n = time step index , i = mesh point index.
The finite difference representation of the momentum balance equation (3.8) is implicit with quasi-linearization of the quadratic terms :

$$(G^{n+1})^2 = 2 \cdot G^{n+1}G^n - (G^n)^2$$

Together with the implicit finite difference representation of the mass balance equation (3.10) it performs a system of linear algebraic equations

$$p_{i+1}^{n+1} = p_i^{n+1} + a_{1i}G_{i+1}^{n+1} + a_{2i}G_i^{n+1} + b_{1i}$$

$$G_{i+1}^{n+1} = G_i^{n+1} + b_{2i} \qquad (3.25)$$

which is solved introducing the Ricatti transformation

$$p = G \cdot r + s \tag{3.26}$$

In this way a simultaneous determination of pressure and mass velocity distribution for parallel channels with pressure drop or inlet mass flow rate boundary conditions is possible. In the case of given total mass flow rate through the core an additional iteration level is necessary. Pressure drop over the channels is corrected in the way :

$$\Delta p^{(j+1)} = \Delta p^{(j)} \left[(m_{tot,0}/m_{tot}^{(j)})^2 \cdot \Theta + 1 - \Theta \right) \tag{3.27}$$

$m_{tot,0}$ is the given total mass flow rate at the core inlet , j is the iteration number and Θ a relaxation parameter (usually $0,5 < \Theta < 1$) ,

$$m_{tot,0} = \sum_k A_k G_{0,k} \ , \tag{3.28}$$

A_k - flow cross section of the assembly (channel) number k.
When cross flow is taken into account , the mass velocities are corrected by following procedure :

$$G^*_{i,k} = \frac{G^{(m)}_{i,k}}{(\Delta p_{i,k})^{1/2} \sum_k \frac{A_k G^{(m)}_{i,k}}{(\Delta p_{i,k})^{1/2}}} \cdot \frac{m_{tot,i}}{} \tag{3.29}$$

$$G^{(m+1)}_{i,k} = \Theta \, G^*_{i,k} + (1-\Theta) \, G^*_{i,k}$$

i - index of axial mesh point , k - index of coolant channel , m - number of iteration , $\Delta p_{i,k} = p_{i,k} - p_{i+1,k}$, the total mass flow rate at the level i is determined by equation (3.14).
Pressure distribution is obtained from equation (3.25).
This iteration procedure is repeated until the condition

$$\max_{i,k} \left| \frac{\Delta p_{i,k} - \Delta p_i}{\Delta p_i} \right| < EPS \quad \text{with } \Delta p_i = 1/NK \sum_k \Delta p_{i,k} \tag{3.30}$$

is satisfied. In this way the conditions (3.13) for cross flow with $\Delta p_{cross} = 0$ are fulfilled.
It can be emphasized , that the iteration procedure for the cross

flow case is as fast as for the case of insulated channels.
The heat conduction equation (3.5) is discretizised introducing effective heat transfer coefficients between radial fuel zones and to the cladding. This coefficients are determined from the exact analytical solution of the steady-state equation with piecewise constant heat conductivity. In this way a good accuracy already for a few fuel zones is reached. In the case of temperature dependent heat conductivity an iterative solution of the heat conduction equation is necessary. For the time dependence the CRANK- NICOLSON-scheme is used.
Iterative procedures are also necessary for the determination of the heat transfer coefficient in the post-critical region (dependence from cladding surface temperature) and the void fraction (dependence of the condensation rate from φ).
After the solution of the heat conduction equation for the fuel rod (using heat fluxes at the cladding surface from previous time step) the heat transfer package is called and new heat transfer coefficients and heat fluxes are determined. For the limitation of heat flux change rates per tims step a time step control procedure is used.

4. Verification of Neutron Flux Calculation Part

Some work carried out on this field was and will be published. Therefore it is mentioned here only. Following calculations were performed:

A 2 - dimensional stationary flux calculations were compared with benchmark solutions for the reactor VVER-440 /1/. The accuracy of the used method is in the order of 0.05 % deviation of the eigenvalue and 1.6 % maximal deviation of assembly power.

B 3 - dimensional stationary results could be compared only with other codes, because a benchmark solution does'nt exist until now. A good accuracy of the code can be assumed for examples of VVER-440 /1/ and VVER-1000 /13/.

C Measured reactivity weights of VVER-440 are compared with calculation of the stationary code HEXNOD23 in Table I. We see that the results of calculations are in the range of experimental accuracy.
In Fig. 2 the critical boron concentrations in dependence from the positions of absorber bank K6 is shown for experiments at hot zero power carried out at unit 5 of NPP Greifswald (GDR). The measured boron concentration is a little higher in comparison to the averaged curve from experiments at several units

VVER-440 in CMEA countries. The calculations performed with data from MAGRU library /3/, underestimate the absorber weight, because it must be assumed that the cross section of absorber assemblies describes the reactivity weight inaccurate, if diffusion theory is used (Fig. 2). Equivalent constants based on flux behaviour near to the absorber boundary gives probably better results. Here the absorption cross section was adjusted to describe the reactivity weight in agreement with measurements. As can be seen also in Fig. 2, the deviations to experiments are smaller. If we compare calculations and measurement, we must notice that the boron concentration is measured with the accuracy of 0.15 g/kg.

D Kinetic experiments at the zero power reactor were used for verification of neutron kinetic part. Results of comparison for 5 representative measurements of 9 experiments during the 3 stages of the years 1986,1987 and 1988 are given in /14/. Reactivities and time behaviour of detector rates at several in core positions were compared with results of DYN3D/M1. Parts of the comparisons are also given in /15,16,17,18,19/.

5. Validation of the FLOCAL Model

For the FLOCAL model validation following activities are carried out:

A validation of separate-effect-models with steady-state experimental results , particularly
-verification and modification of the used subcooled boiling model by MOLOCHNIKOV /5/,
-calculation of critical heat flux experiments in tubes and rod bundles /20,21,22/,
-comparison with wall temperature measurements in the post-crisis region /20/.
The Figures 4 and 5 show some results of subcooled boiling calculations in comparison with experimental data from literature /23/ and demonstrate the improving effect of the boiling model modification made. Fig. 6 shows an example for wall temperature calculation for the BENNETT experiments , mentioned in /20/. For tube geometry the BIASI critical heat flux correlation gives the best prediction of boiling crisis onset. The MIROPOLSKIJ heat transfer correlation gives satisfactory results for post-critical wall temperatures.

B Comparison with other codes
Comparison with similar codes were carried out on some test cases simulating loss-of-flow conditions and power excursions.

Fig. 7 shows the results of an international benchmark problem involving a transient initiated by instantaneous application of a uniform heat source to a section of a 7 m long pipe /26/, obtained by the benchmark code MECA and FLOCAL. The code MECA includes pressure wave propagation which is not considered in FLOCAL.

For the cross flow model comparisons with exact solutions for sample problems /24/ were done. It was seen , that the effect of flow diversion from hot to cool channels is underestimated by the FLOCAL model , but a rough estimation of cross flow effects in comparison with the approximation of isolated channels is possible. The outlet vapour mass fraction of the hottest channel is 18.4 % for the exact solution, 16 % for FLOCAL and 34.6 % for isolated channels. FLOCAL results were also compared with calculations for a loss of main pump power transient for a VVER-440 , carried out by the help of code COBSOF, which is a modified version of the code COBRA-IIIC/25/. While COBSOF gives a minimum DNB-ratio for the hottest rod during the transient of 2.80, the FLOCAL values are 2.85 taking into account crossflow and 2.60 without cross flow. Here the same CHF-correlation is used (OKB without formfactor). Investigations have shown that model uncertainties (use of several CHF-correlations, gas gap heat transfer modeling) exceed the cross flow effect significantly , when the differences in thermal conditions for several coolant channels are not very large.

C Calculations to RIA experiments from literature

Calculations to fuel rod behaviour during fast power excursions play an important role in the verification of a thermohydraulic model for reactivity-initiated transients analysis. Fig. 8 shows calculated temperature curves obtained by FLOCAL in comparison with results from RIA experiments /27/. In the experiments the influence of subcooling on wall temperature behaviour was investigated. The calculational results agree fairly well with the experimental data , with the exception of a coolant subcooling of 80 K. In this case the experimental wall temperatures are remarkably underestimated by FLOCAL. Calculations for another RIA experiment /28/ with a coolant subcooling of 80 K show a better qualitative agreement with the measured wall temperature behaviour (see Fig. 9). This discrepancies could not be removed by some variations of the heat transfer model. We see that on the basis of the contradictory results for the considered experiments no unambiguous recommendation for one of the investigated heat transfer models can be given. Further work has to be done in this direction.

D Sensitivity studies

For investigation of the influence of model uncertainties some sensitivity studies on test cases were carried out . In this studies gas gap model and post-crisis heat transfer model were varied. One of these test cases was EXKURS-F , an idealized example for a power pulse at VVER-conditions. In this test case a power peak of variable relative heigth F and half-life time 0,4 s starting from normal stationary state at burn-up A is assumed. The input data for the gas gap model for several values of A were obtained from the code STOFFEL /12/. As a result of this investigations following conclusions were pointed out:

-The use of different critical heat flux correlations gives no significant differences for the considered process, because the heat transfer crisis occurs very fast.

-The discrepancies between several non-equilibrium corrections of the post-crisis heat transfer coefficient are not so large for power reactor conditions (high pressures , low or medium subcooling) as for the RIA experiments conditions (low pressure). Differences between maximum cladding temperature values calculated by the help of several investigated models are lower than 75 K.

-The choice of Leidenfrost point correlation is of significant influence. The used correlation (3.21) gives conservative results in comparison with the other investigated models. The differences in time until rewetting due to different Leidenfrost points cause differences in oxide layer thickness up to 100 % (between 19 and 38 µm).

-An underestimation of the gas gap conductance is not necessarily conservative. It causes higher fuel centerline temperatures , but a less extent of boiling crisis and lower cladding temperatures. Plastic deformation of cladding in the high temperature region leads to intensification of the heat transfer by closure of the gas gap.

-The model is able to predict qualitatively the fuel rod failure. The calculated failure limits for the test case EXKURS agree with criteria given in /29/ (fuel rod failure at fuel enthalpy values $h \gtrsim 250$ cal/g for fresh fuel , decrease of this limit to $h \gtrsim 100$ cal/g for depleted fuel with A=25000 MWd/t U). Some results of the test case calculation are shown in Table II.

The results of the described first validation activities for the thermohydraulic module FLOCAL demonstrate the applicability

of the code for reactivity-initiated transients analysis , but also show the need of further model improvements.

6. Range of Application

The range of application of the code DYN3D/M2 is given by following characteristics:

- calculations of reactivity transients can be carried out by assuming intact core geometry
- determination of the stationary state
- reactivity changes can be induced by
  - motion of control rods
  - changes of inlet coolant temperatures of fuel assemblies or coolant flow rate
  - changes of boron concentration
- depending on the core symmetriy during the transient process calculations with 30 degree reflectional, 60 degree rotational, 120 degree rotational, 180 degree reflectional (2 types) symmetries and for the whole core are possible.
- inlet coolant temperatures of fuel assemblies, mass flow rate or pressure drop and system pressure must be given (constant or as functions of time)
- a limit for the fuel rod model is fuel or cladding melting
- the thermohydraulics works from one phase liquid flow up to superheated steam (flow reversal can't be treated at present)

The code was applied to a rod ejection accident at a VVER-1000 reference core/19/. Regarding a feedback induced reactivity transient during a LOCA of VVER-440 at hot zero power the dependence of feedback reactivities from the thermohydraulic state was calculated with the stationary part of this code. The obtained reactivity behaviour was used for the point model of code RELAP4/MOD6/30/.

Appendix A:

Inner Nodal Relations

With help of the assumption

$$\varphi_g(\vec{r}) = \Phi_g \cdot \psi_g(x,y) \cdot f_g(z) \tag{A1}$$

and the normalizations

$$\begin{aligned} 1/F_{HEX} \cdot \int_{F_{HEX}} dF \cdot \psi_g(x,y) &= 1 \\ 1/\Delta z \cdot \int_{\Delta z} dz \cdot f_g(z) &= 1 \end{aligned} \tag{A2}$$

with
F_{HEX} - area of the hexagonal assemblies
Δz - height of node
one obtains by inserting in the neutron diffusion equations (2.1) and integration over Δz the following 2-dimensional diffusion equation

$$\begin{aligned} -D_1 \Delta_{xy} \chi_1(x,y) + \Sigma_{a1} \cdot \chi_1(x,y) &= \frac{1}{k_{eff}} \sum_{g=1}^{2} \nu\Sigma_{fg} \cdot \chi_g(x,y) \\ -D_2 \Delta_{xy} \chi_2(x,y) + \Sigma_{a2} \cdot \chi_2(x,y) &= \Sigma_s \cdot \chi_1(x,y) \end{aligned} \tag{A3}$$

where

$$\begin{aligned} \chi_g(x,y) &= \Phi_g \cdot \psi_g(x,y) \\ \Sigma_{a1} &= \Sigma_r + D_1 B_{z,1}^2 \\ \Sigma_{a2} &= \Sigma_a + D_2 B_{z,2}^2 \end{aligned} \tag{A4}$$

The transversal bucklings are calculated from the mean partial currents by

$$D_g B_{z,g}^2 = \frac{1}{\Delta z \cdot \Phi_g} \cdot (j_{g,l}^{out} - j_{g,l}^{in} + j_{g,u}^{out} - j_{g,u}^{in}) \tag{A5}$$

We define

$$\chi_g(x,y) = e_g \cdot p(x,y) \qquad (A6)$$

where $p(x,y)$ is a solution of the 2-dimensional Helmholtz equation

$$\Delta_{xy}(x,y) + B^2 \cdot p(x,y) = 0 \qquad (A7)$$

Inserting assumption (A6) with Eq. (A7) in Eqs. (A3), we find two values of bucklings B^2 by solving the corresponding quadratic equation. $\chi_g(x,y)$ can be composed by the two solutions for fundamental (index F) and transient (index T) bucklings B^2.

$$\chi_g(x,y) = e_{g,F} \cdot p_F(x,y) + e_{g,T} \cdot p_T(x,y) \qquad (A8)$$

The relations between $e_{2,F}/e_{1,F}$ and $e_{2,T}/e_{1,T}$ are given by

$$e_2/e_1 = \Sigma_s/(\Sigma_{a2} + D_2 B^2) \qquad (A9)$$

if B^2 is replaced by the corresponding values B_F^2 or B_T^2.
Introducing polar co-ordinates (r,φ) we can expand the solutions of the Helmholtz equation in a series of Bessel functions

$$p_F(x,y) = A_0^F \cdot J_0(B_F r) + \sum_{l=1}^{\infty} [A_l^F \cos(l\varphi) + C_l^F \sin(l\varphi)] \cdot J_l(B_F r) \qquad \text{for } B_F^2 \geq 0$$

$$p_T(x,y) = A_0^T \cdot I_0(B_T r) + \sum_{l=1}^{\infty} [A_l^T \cos(l\varphi) + C_l^T \sin(l\varphi)] \cdot I_l(B_T r) \qquad \text{for } B_T^2 < 0 \quad \text{and} \quad B_T = (-B_T^2)^{1/2} \qquad (A10)$$

where J_l are the Bessel functions of first kind and I_l the modified Bessel functions /31/. Here we assumed $B_F^2 > 0$ and $B_T^2 < 0$, but in the general case that is not necessary and the typ of Bessel functions depends only from the corresponding value of B^2. Inserting the expansions (A10) in the Eq. (A8), we can determine the coefficients A_0^F and A_0^T from the mean nodal fluxes Φ_g, providing that we integrate instead over the area of hexagon approxi-

mately over the cycle with the mean radius $\bar{r}$, defined by

$$\bar{r} = (F_{HEX}/\pi)^{1/2} \tag{A11}$$

The next lowest coefficients of the expansion are determined by the 6 incoming partial currents $j^{in}_{g,i}$ at the 6 surfaces of hexagon (Fig. 1). Calculating the mean values of partial currents on the related face, we integrate in the expansions, derived from Eqs. (A10) for the partial currents, also over the mean radius $\bar{r}$. Besides A_0 the coefficients A_1, A_2, A_6, C_1, C_2 and C_3 give linearly independent contributions to the incoming currents. Therefore these coefficients of fundamental and transient part can be expressed by the incoming currents. After that the coefficients can be used for the expressions of outgoing partial currents $j^{out}_{g,i}$ and one obtains after troublesome calculations, being not demonstrated here, the wanted relations (2.7)

$$j^{out}_{g,i} = \sum_{g'=1}^{2} P_{gg'} \cdot \Phi_{g'} + \sum_{i'=1}^{6} \sum_{g'=1}^{2} W^{ii'}_{gg'} \cdot j^{in}_{g',i'} \tag{A12}$$

with

$$\begin{bmatrix} P_{11} & P_{12} \\ P_{21} & P_{22} \end{bmatrix} = \frac{1}{4} \begin{bmatrix} 1 & \epsilon_T \\ \epsilon_F & 1 \end{bmatrix} \cdot \begin{bmatrix} H_F & 0 \\ 0 & H_T \end{bmatrix} \cdot \begin{bmatrix} 1 & \epsilon_T \\ \epsilon_F & 1 \end{bmatrix}^{-1} \tag{A13}$$

and $\epsilon_F = e_{2,F}/e_{1,F}$ and $\epsilon_T = e_{1,T}/e_{2,T}$.
If for example $B^2_F > 0$ and $B^2_T < 0$ is assumed, we obtain

$$H_F = (B_F\bar{r}) \cdot J_0(B_F\bar{r})/J_1(B_F\bar{r})$$

and (A14)

$$H_T = (B_T\bar{r}) \cdot I_0(B_T\bar{r})/I_1(B_T\bar{r})$$

Considering the $W^{i,i'}_{g,g'}$ regarding the indizes i,i' as matrices

$\{W_{g,g'}\}$, we can write

$$\{W_{gg'}\} = \begin{bmatrix} R_{gg'} & S_{gg'} & T_{gg'} & U_{gg'} & T_{gg'} & S_{gg'} \\ S_{gg'} & R_{gg'} & S_{gg'} & T_{gg'} & U_{gg'} & T_{gg'} \\ T_{gg'} & S_{gg'} & R_{gg'} & S_{gg'} & T_{gg'} & U_{gg'} \\ U_{gg'} & T_{gg'} & S_{gg'} & R_{gg'} & S_{gg'} & T_{gg'} \\ T_{gg'} & U_{gg'} & T_{gg'} & S_{gg'} & R_{gg'} & S_{gg'} \\ S_{gg'} & T_{gg'} & U_{gg'} & T_{gg'} & S_{gg'} & R_{gg'} \end{bmatrix} \qquad \text{(A15)}$$

In consequence of the hexagonal symmetry the matrices consist in four different elements only, given by

$$\begin{aligned} R_{gg'} &= 1/6(\ 2K^1_{gg'} + 2K^2_{gg'} + K^3_{gg'} - \delta_{gg'}) \\ S_{gg'} &= 1/6(\ K^1_{gg'} - K^2_{gg'} - K^3_{gg'} - \delta_{gg'}) \\ T_{gg'} &= 1/6(-K^1_{gg'} - K^2_{gg'} + K^3_{gg'} - \delta_{gg'}) \\ U_{gg'} &= 1/6(-2K^1_{gg'} + 2K^2_{gg'} - K^3_{gg'} - \delta_{gg'}) \end{aligned} \qquad \text{(A16)}$$

and

$$\begin{bmatrix} K^n_{11} & K^n_{12} \\ K^n_{21} & K^n_{22} \end{bmatrix} = \begin{bmatrix} a^{n+}_{1,F} & \epsilon_T a^{n+}_{1,T} \\ \epsilon_F a^{n+}_{2,F} & a^{n+}_{2,T} \end{bmatrix} \cdot \begin{bmatrix} a^{n-}_{1,F} & \epsilon_T a^{n-}_{1,T} \\ \epsilon_F a^{n-}_{2,F} & a^{n-}_{2,T} \end{bmatrix}^{-1} \qquad \text{(A17)}$$

where

$$\begin{aligned} a^{1+}_{g,F} &= \frac{\sqrt{3}}{8\pi}\{3J_1(B_F\bar{r}) \pm D_g B_F[3\sqrt{3}J_1(B_F\bar{r})/(B_F\bar{r}) - (3/2\sqrt{3}+\pi)J_0(B_F\bar{r})]\} \\ a^{2+}_{g,F} &= \frac{1}{16\pi}\{3\sqrt{3}J_2(B_F\bar{r}) \pm D_g B_F[16J_2(B_F\bar{r})/(B_F\bar{r}) - 10J_1(B_F\bar{r})]\} \\ a^{3+}_{g,F} &= \frac{8\sqrt{3}}{16\pi}\{8\sqrt{3}/9J_3(B_F\bar{r}) \pm D_g B_F[6J_3(B_F\bar{r})/(B_F\bar{r}) - 3J_2(B_F\bar{r})]\} \end{aligned} \qquad \text{(A18)}$$

and $\delta_{gg'}$ - Kroneckers symbol

The same relations are obtained also for the transient terms. In the case of $B^2 < 0$ the ordinary Bessel functions J_1 must be replaced by the modified functions I_1.

Now the required relations between mean partial currents and fluxes of the 2-dimensional hexagonal problem are found and we regard the axial problem. The equations are obtained after insertion of (2.6) in Eqs. (2.1) with (2.2) and integrations over the

area of hexagons F_{HEX}.

$$-D_1\frac{d^2}{dz^2}h_1(z) + (\Sigma_r + D_1B^2_{r,1})\cdot h_1(z) = \frac{1}{k_{eff}}\sum_{g=1}^{2}\nu\Sigma_{fg}\cdot h_g(z)$$

$$-D_2\frac{d^2}{dz^2}h_2(z) + (\Sigma_a + D_2B^2_{r,2})\cdot h_2(z) = \Sigma_s\cdot h_1(z) \qquad (A19)$$

with

$$h_g(z) = \Phi_g\cdot f_g(z)$$

and the transversal bucklings

$$D_gB^2_{r,g} = \frac{2}{3d\Phi_g}\sum_{i=1}^{6}(j^{out}_{g,i} - j^{in}_{g,i}) \qquad (A20)$$

where d is the distance of parallel sides of hexagons.
The equations will be treated with methods similar to those used for rectangular geometry /2/. The neutron flux $h_g(z)$ is expanded in polynomials up to the 4^{th} order

$$h_g(z) = \Phi_g\xi_0(w) + 1/2[h_g(z_u) - h_g(z_l)]\,\xi_1(w) + (\Phi_g - 1/2[h_g(z_u) + h_g(z_l)])\xi_2(w) + C_{3,g}\xi_3(w) + C_{4,g}\xi_4(w)$$

where

(A21)

$$\xi_0(w) = 1$$
$$\xi_1(w) = 2w - 1$$
$$\xi_2(w) = 6w(1 - w) - 1$$
$$\xi_3(w) = 6w(1 - w)(2w - 1)$$
$$\xi_4(w) = 6w(1 - w)(5w^2 - 5w + 1)$$

$$w = (z - z_l)/\Delta z$$
$$z_l \le z \le z_l + \Delta z = z_u$$

z_l and z_u are the axial co-ordinates at the lower and upper boundary. With help of Fick's law Eq. (2) for the net currents at lower and upper surface of node and

$$h_g(z_k) = 2(j^{out}_{g,k} + j^{in}_{g,k}) \qquad (A22)$$

we obtain the relations (2.8) between partial currents and mean fluxes

$$j^{out}_{g,u} = \alpha_g(\Phi_g + C_{g,4}) - a_g \cdot j^{in}_{g,u} - b_g \cdot j^{in}_{g,l} + \eta_g \cdot C_{3,g}$$
$$j^{out}_{g,l} = \alpha_g(\Phi_g + C_{g,4}) - b_g \cdot j^{in}_{g,u} - a_g \cdot j^{in}_{g,l} - \eta_g \cdot C_{3,g} \qquad \text{(A23)}$$

with

$$\alpha_g = \frac{6x_g}{12x_g+1}$$

$$a_g = \frac{48x_g^2-1}{(12x_g+1)(4x_g+1)}$$

$$b_g = \frac{8x_g}{(12x_g+1)(4x_g+1)} \qquad \text{(A24)}$$

$$\eta_g = \frac{6x_g}{4x_g+1}$$

$$x_g = D_g/\Delta z$$

By weigthing the Eq. (A19) by ξ_1 and ξ_2 and integrating over Δz algebraic equations for the higher coefficient $C_{3,g}$

$$(a_{11}+60D_1/\Delta z^2)\cdot C_{3,1} + a_{12}\cdot C_{3,2} = -5/6\{a_{11}[h_1(z_u)-h_1(z_l)] + a_{12}[h_2(z_u)-h_2(z_l)]\}$$
$$a_{21}\cdot C_{3,1} + (a_{22}+60D_2/\Delta z^2)\cdot C_{3,2} = -5/6\{a_{21}[h_1(z_u)-h_1(z_l)] + a_{22}[h_2(z_u)-h_2(z_l)]\} \qquad \text{(A25)}$$

and similar for $C_{4,g}$

$$(a_{11}+140D_1/\Delta z^2)\cdot C_{4,1} + a_{12}\cdot C_{4,2} = 7/3\{a_{11}(\Phi_1-1/2[h_1(z_u)+h_1(z_l)]) + a_{12}(\Phi_2-1/2[h_2(z_u)+h_2(z_l)])\}$$

$$a_{21}\cdot C_{4,1} + (a_{22}+140D_2/\Delta z^2)\cdot C_{4,2} = 7/3\{a_{21}(\Phi_1-1/2[h_1(z_u)+h_1(z_l)]) + a_{22}(\Phi_2-1/2[h_2(z_u)+h_2(z_l)])\} \quad (A26)$$

with

$$\begin{aligned} a_{11} &= \Sigma_r + D_1 B_{r,1}^2 - \nu\Sigma_{f1}/k_{eff} \\ a_{12} &= -\nu\Sigma_{f2}/k_{eff} \\ a_{21} &= -\Sigma_s \\ a_{22} &= \Sigma_a + D_2 B_{r,2}^2 \end{aligned} \quad (A27)$$

are given.

References

/ 1/ Grundmann U.
HEXNOD23 - a Two- and Three-Dimensional Nodal Code for Neutron Flux Calculation of Thermal Reactors with Hexagonal Geometry , Rep. ZfK - 557,Rossendorf 1985

/ 2/ Finnemann H.
Nodal Expansion Method for the Analysis of Space-Time-Effects in LWRs. Proceedings of a Specialists Meeting on "The Calculation of 3-dimensional Rating Distributions in Operating Reactors" , Paris 1979, p. 257-281

/ 3/ Agthe G., H. - J. Kretzschmar
Die Gruppenparameterbibliothek MAGRU - EC und das zugehörige Verwaltungsprogramm PREPAR - EC
RPT - 3/88, common rep.of KKAB Berlin and ZfK Rossendorf, Rossendorf 1988

/ 4/ Poljanin,L.N.,M.Ch.Ibragimov,G.P.Sabeljev
Teploobmen v jadernykh reaktorakh
Moskva:Ehnergoatomizdat,1982

/ 5/ Molochnikov,Yu.S. et al.
Teploehnergetika 1982 , Nr.7 , p.47

/ 6/ Astachov,V.I.,Yu.A.Bezrukov,S.A.Logvinov
CMEA-Seminar "Teplofizika - 82",Karlovy Vary,4.-6.5.1982, Proc. Vol. 4, p.168

/ 7/ Osmachkin,V.S.
CMEA-Seminar "Teplofizika - 78",Budapest,20.-23.3.1978, Proc. Vol. 1, p.27

/ 8/ L.Biasi et al.
Energia Nucleare 14 , Nr.9 , Sept.1967

/ 9/ Huhn,J.,J.Wolf
Zweiphasenströmung gasförmig - flüssig
Leipzig: VEB Fachbuchverlag, 1975

/10/ Heat Transfer Correlations in Nuclear Safety Calculations Vol. I,II , Nord 6/1985 , Risö - M - 2504

/11/ Gotovskij,M.A. et al.
The influence of fluid subcoling on the minimum temperature difference in film boiling (in Russian),
in Compendium "Teploobmen v ehnergooborudovanii AEhS", p.156-165 , Moskva: Nauka,1986

/12/ Reinfried,D.: Zur mathematischen Modellierung des Bestrahlungsverhaltens von Druckwasserreaktorbrennstäben , Doctor Thesis A , AdW der DDR , ZfK Rossendorf , 1985

/13/ Kujal B.,Jaderna Energie 35 (1989), pp. 41-45 (in Czech)

/14/ Grundmann U., J.Hadek
Calculation of Neutron Kinetic Experiments at the LR-0 Reactor with the 3- dimensional Code DYN3D/M1
Submitted to journal Kernenergie

/15/ Grundmann U., J. Cermak, J. Hadek
Validation of the 3 - dimensional Neutron Kinetic code HEXDYN3D by Use of the Experiments at the LR-0 Reactor (in Russian)
Rep. UJV 8191-R,A, Rez, 1987

/16/ Grundmann U., J. Hadek
Validation of the 3-dimensional Neutron Kinetics Code HEXDYN3D by use of the 2nd stage of Space - Time - Kinetics Experiments at the LR-0 Reactor (in Russian)
Rep. UJV 8578 R,A, Rez 1988

/17/ Hadek J., U. Grundmann
Rod-drop in the 55 Fuel Assemblies Active Core of the LR-0 Reactor. Comparisons of Calculations and Experiments (in Russian)
Rep. UJV 8855 R, Rez, 1989

/18/ Rypar V. et. al.
Neutron Kinetic Investigation at the Zero Power Reactor LR-0
to be published in Nucl. Sci. Engng.

/19/ Grundmann U., U. Rohde
DYN3D/M2 - a Three-Dimensional Dynamic Code for Cores with Hexagonal Geometry, paper presented at the iaea TCM on Computer Aided Safety Analysis, Berlin, 17.-21. 04. 1989

/20/ Kolev,N.N.
Nucl.Eng.Des. 85 (1985) , p.217-237

/21/ Logvinov,S.A. et al.
CMEA-Seminar "Teplofizika - 84" , Varna , Oct.1984
Proc. Vol. 2 , p.115

/22/ Wolter,W.
CMEA-Seminar "Teplofizika - 84" , Varna , Oct.1984
Proc. Vol. 2 , p.1

/23/ Bartolomej,G.G. et al.
Teploehnergetika 1982 , Nr.3 , p.20

/24/ Huhn,J.
Kernenergie 32 (1989) 5 , p.193-198

/25/ Sabotinov,L.
Thermal-Hydraulic Parameters in the Reactor Core of VVER-440 (B-230) at Loss of Main Pump Power
Paper presented at IAEA TC/Workshop on Computer-Aided Safety Analysis , Berlin , 17-21 April 1989

/26/ Hancox,W.T.,S.Banerjee
Nucl. Sci. Eng. 64 (1977) , p.106-123

/27/ Ohnishi,N.,K.Ishijima,S.Tanzawa
Nucl. Sci. Eng. 88 (1984) , p.331-341

/28/ Asmolov,V.G. et al.
Kernenergie 30 (1987) , p.299-304

/29/ Courtright,E.L.
A Survey of Potential Light Water Reactor Fuel Rod Failure Mechanisms and Damage Limits
NUREG/CR - 1132 (PNL - 2787) , July 1979

/30/ Grundmann U., U. Rohde, H. Wand
Untersuchungen zum ATWS-Störfall "Großes Leck bei Null-leistung" für den WWER-440
RPT - 5/89, internal rep., ZfK Rossendorf 1989

/31/ G. N. Watson
Theory of Bessel Functions
University Press, Cambridge 1958

Table I : Reactivity ϱ (%) of control rod banks of VVER-440 reactor

bank	ϱ_{exp} unit 2	ϱ_{exp} unit 3	ϱ_{calc} HEXNOD23
K6	1.8 ± 0.10	1.83±0.13	1.74
K5	0.48± 0.01	0.49±0.005	0.44
K3,K4	5.40± 0.53	5.12±0.35	5.14
K2	1.39± 0.19	–	1.20

Table II : Results of investigation of the power pulse test case EXKURS by FLOCAL

parameters of test case	energy depos. in fuel /calg^{-1}/	max. fuel temp. /°C/	max. wall temp. /°C/	time of full re-wetting /s/	fuel rod behaviour
A=0 ,F=30	109	1730	821	15.6	closure of gap by plastic def.
A=0 ,F=75	202	2653	1310	18	starting cladding oxidation
A=0 ,F=90	233	2877	1644	>20	oxide layer 20µm, starting fuel melting
A=0,F=120	252	>2850	>1850	–	extensive fuel and cladding melting
A=20,F=30	123	1942	841	9.8	fuel-cladding contact $\sigma_{cont} < \sigma_Y$
A=25,F=30	122	1920	805	9.0	possible cladding rupture $\sigma_{cont} > \sigma_Y$

F = height of power pulse relative to stationary state

A = burnup in 10^4 MWd/t U

Fig. 1: Hexagon with partial currents and polar co-ordinate system

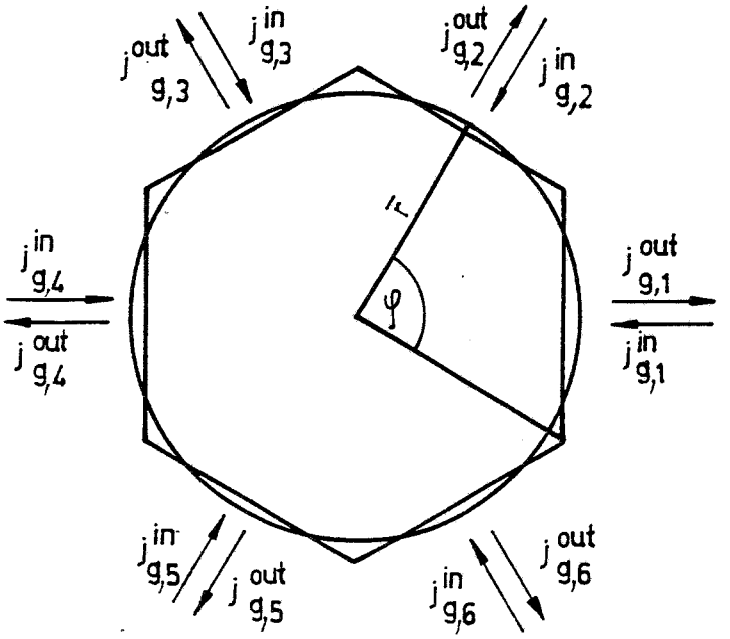

Fig. 2 : VVER-440: C/E – comparison of critical states
(zero power temperature T = 260 deg c)

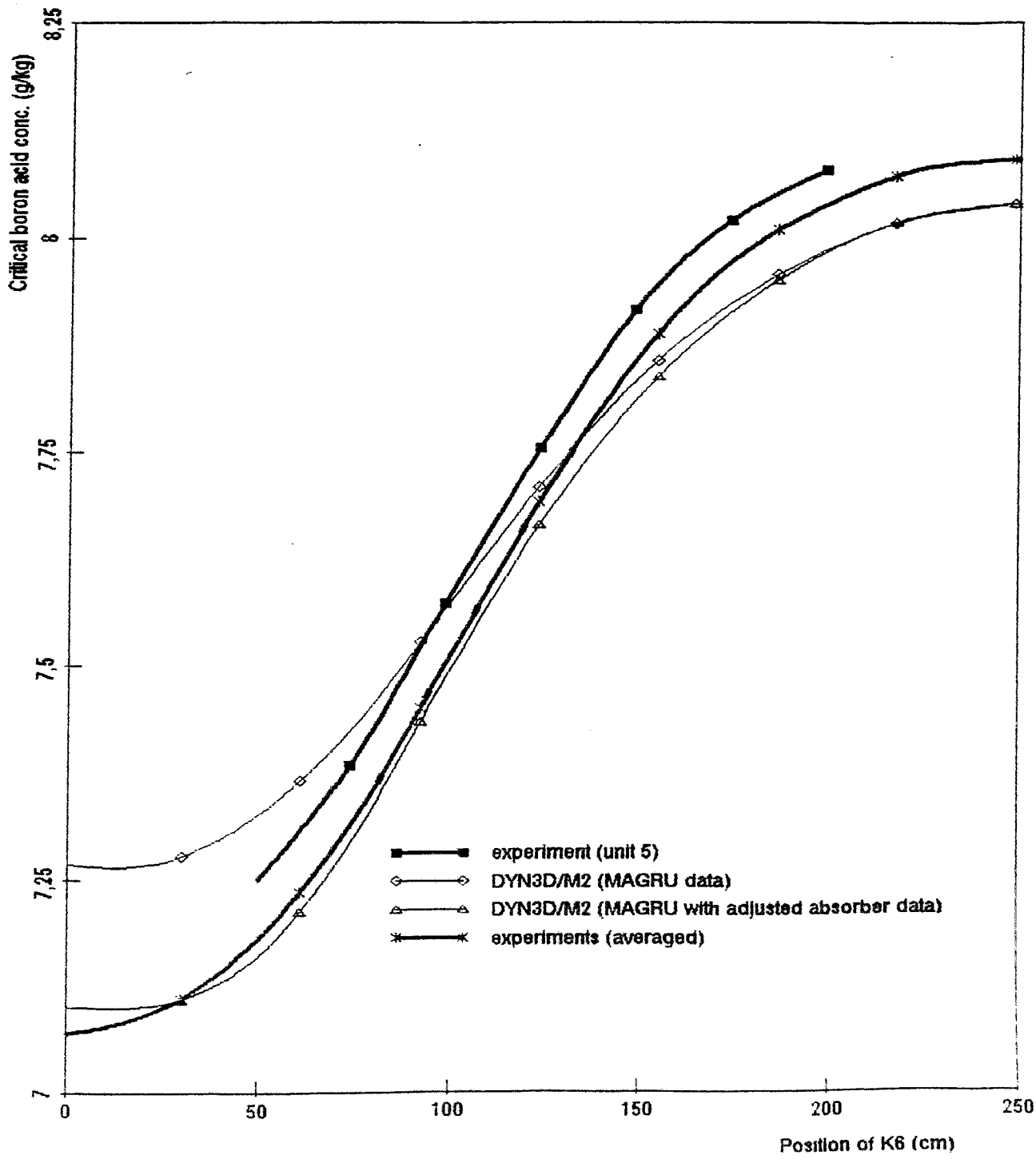

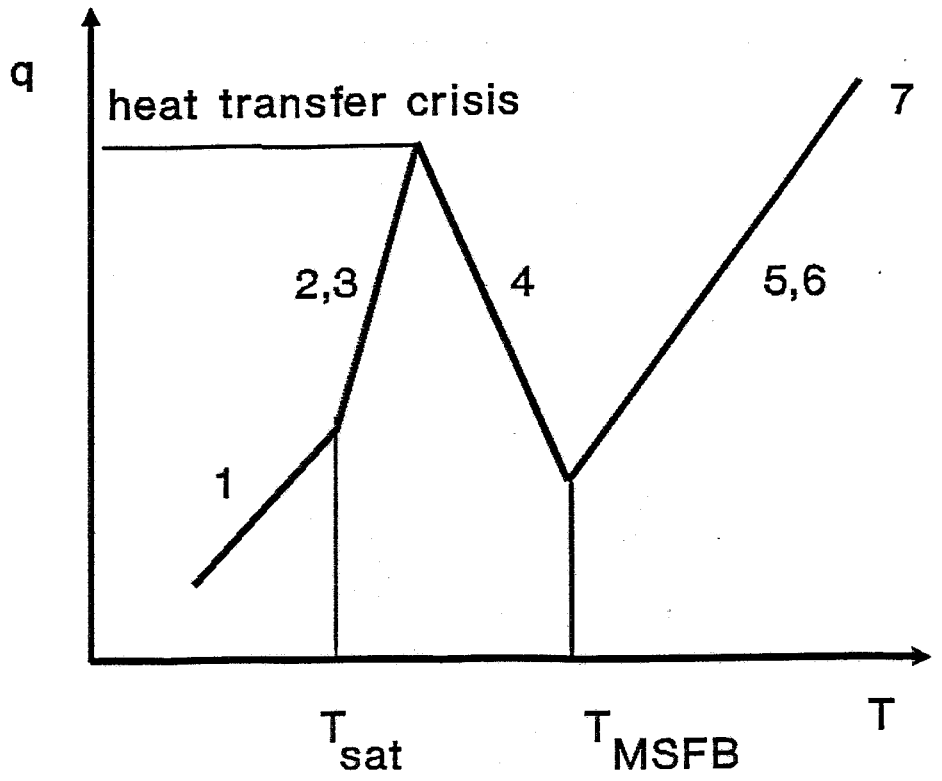

1 one-phase liquid convection
2 boiling heat transfer
3 convection in annular flow
4 transition boiling
5,6 film boiling
(inverted annular or dispersed flow)
7 convection to superheated steam

Fig.3: Heat transfer logic

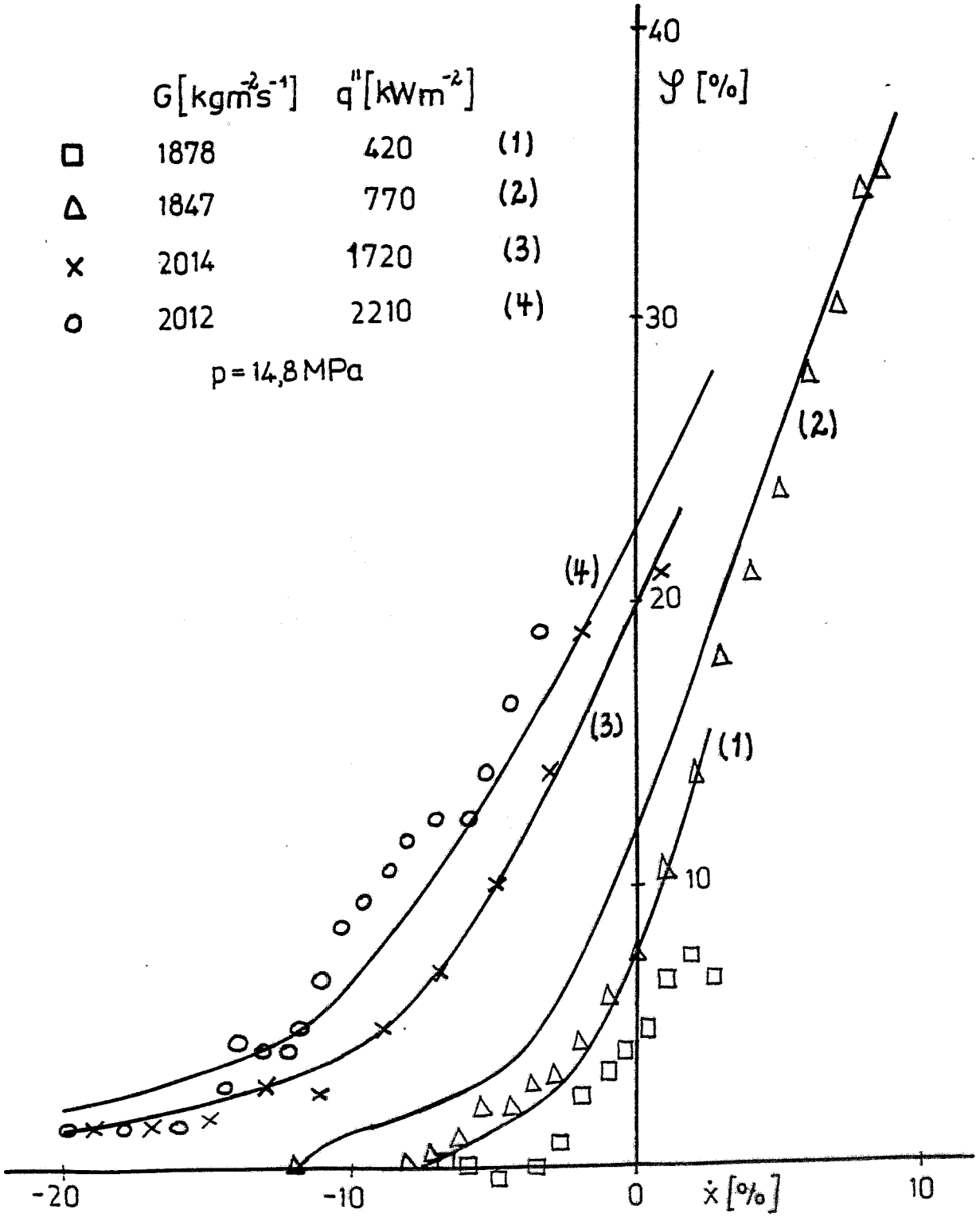

Fig. 4 FLOCAL calculations to subcooled boiling experiments with variation of heat flux

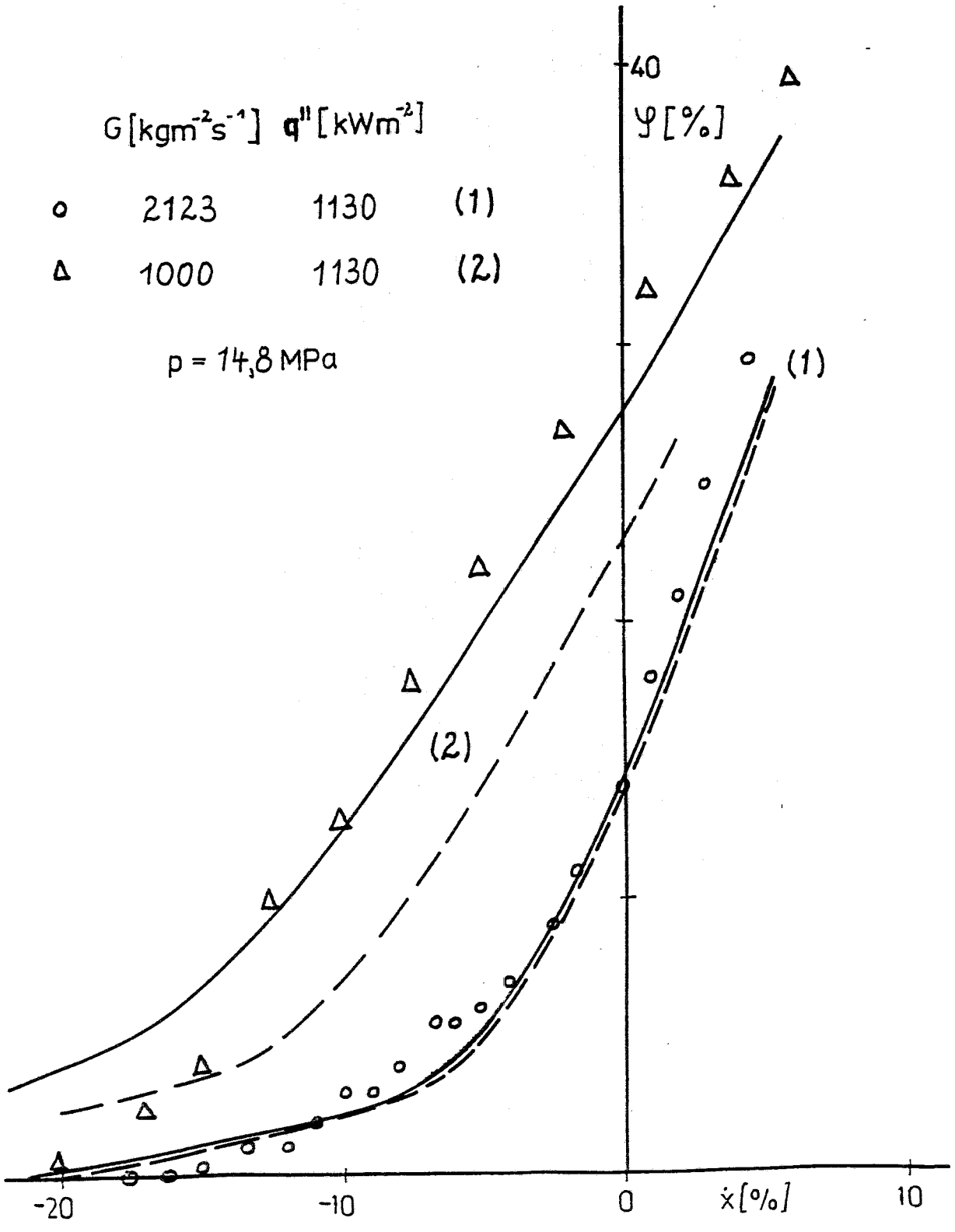

Fig. 5 FLOCAL calculations to subcooled boiling experiments with variation of mass flow rate

- - - - - - original MOLOCHNIKOV boiling model

——— modified model used in FLOCAL

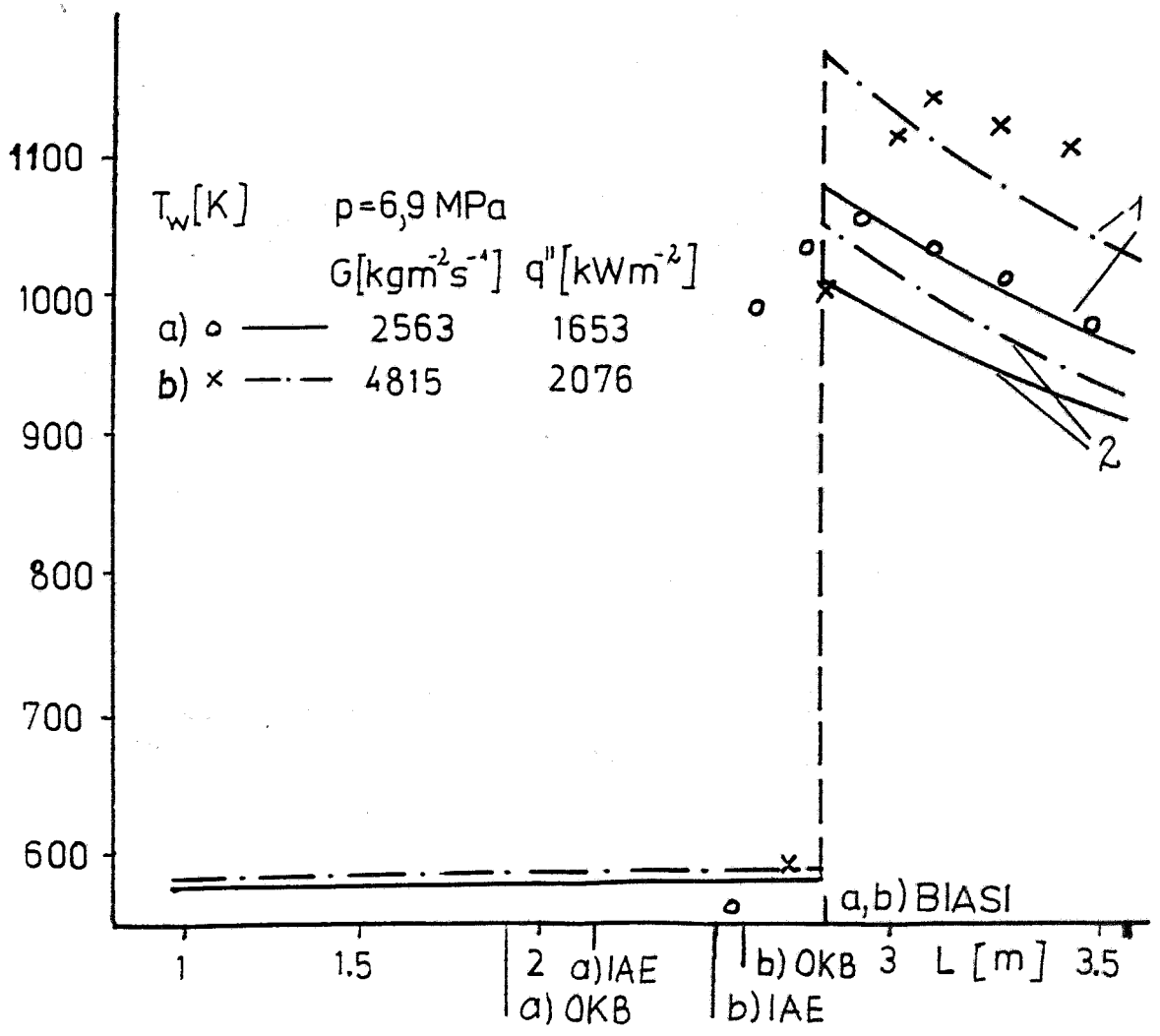

Fig. 5 FLOCAL calculations to post-crisis heat transfer experiments by BENNETT

Boiling crisis onset determined by several correlations is marked on the x - axis , temperatures were obtained using heat transfer coefficients by

1 - MIROPOLSKIJ , 2 - GROENEVELD

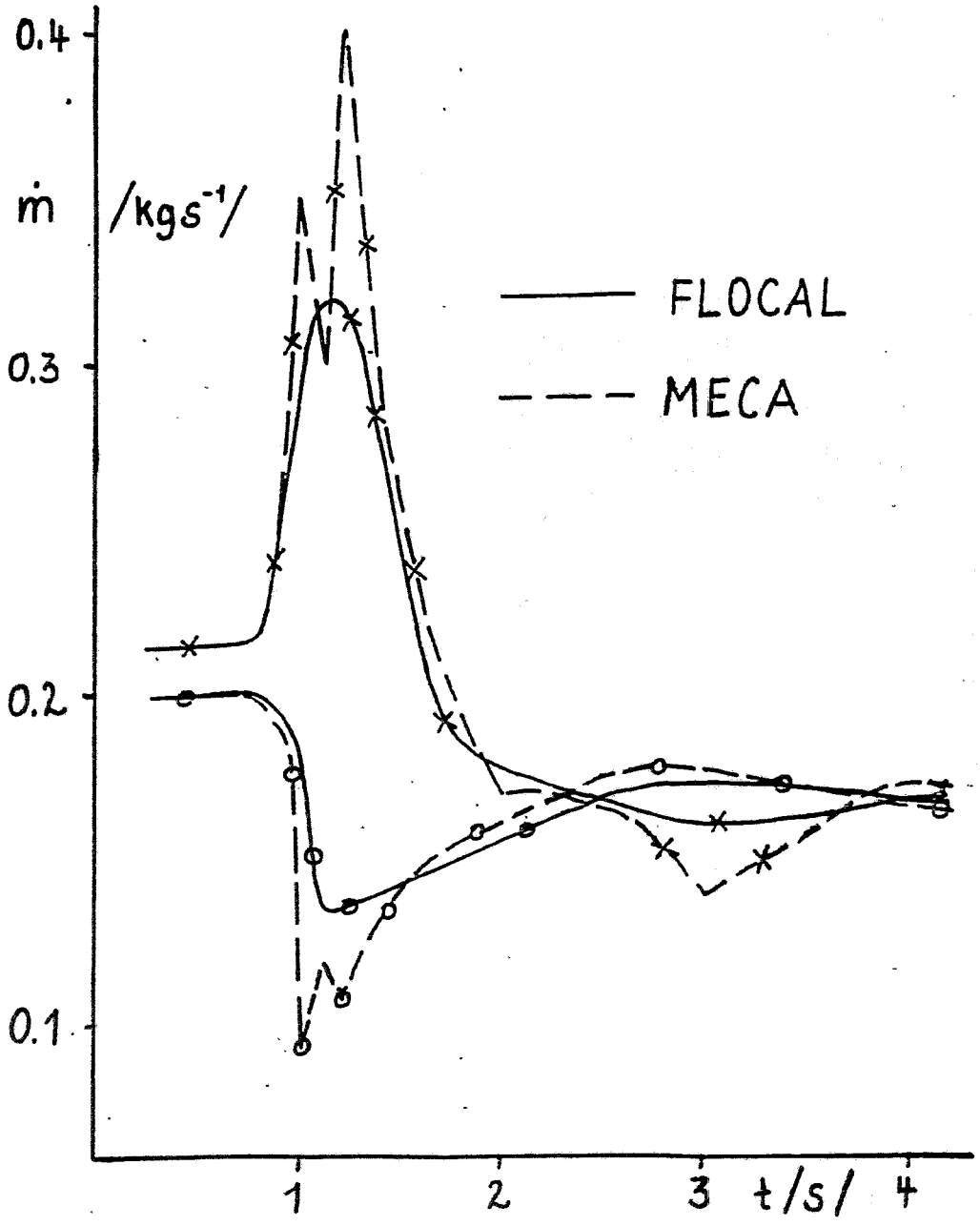

Fig. 7 FLOCAL results (mass flow rate $\dot{m}$) for a benchmark problem involving a transient initiated by instantaneous heat supply to a section of a pipe /26/

x x x exit flow rate

o o o inlet flow rate

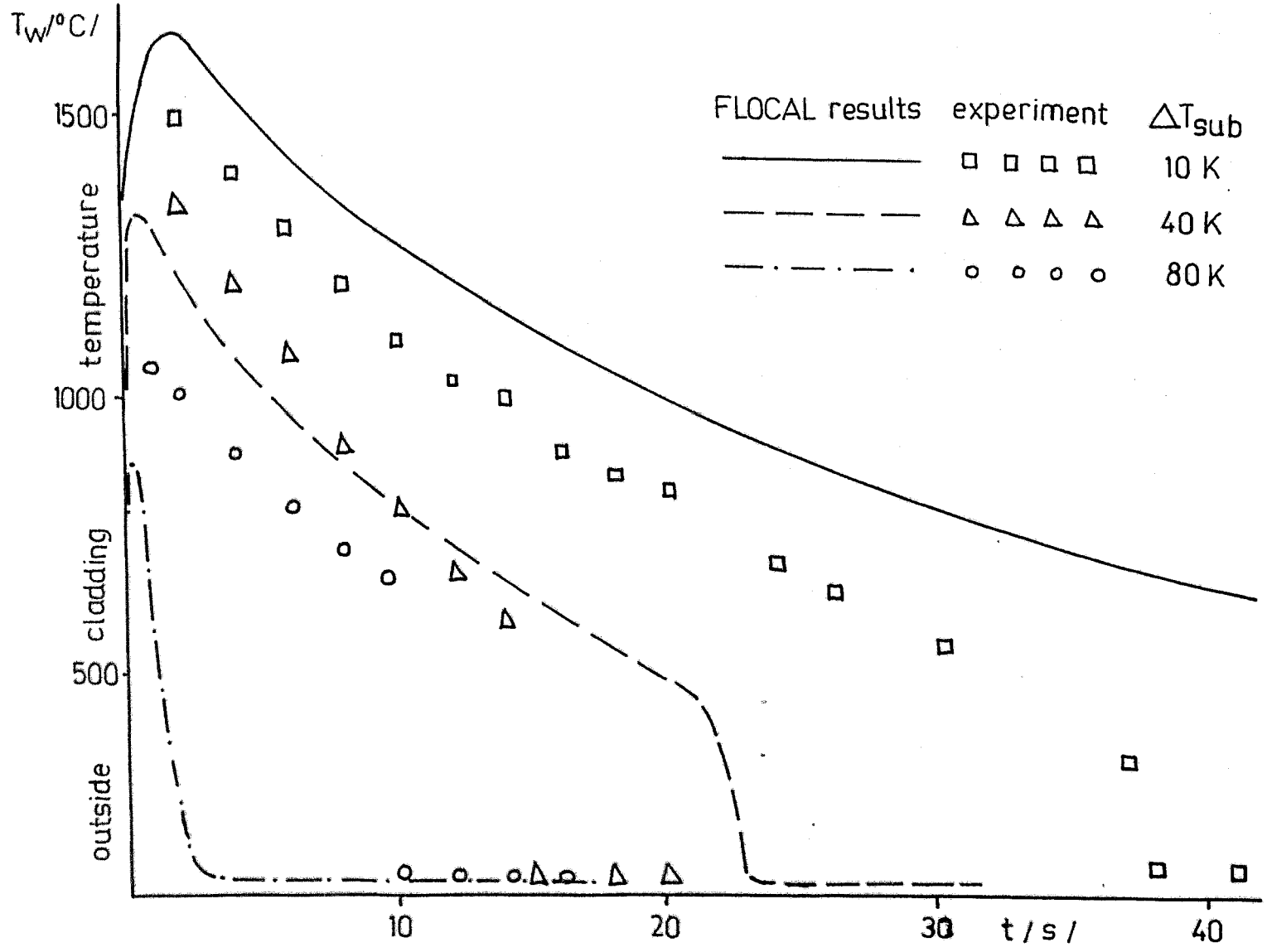

Fig. 8 FLOCAL calculations for RIA experiments /27/ with variation of subcooling ΔT_{sub}

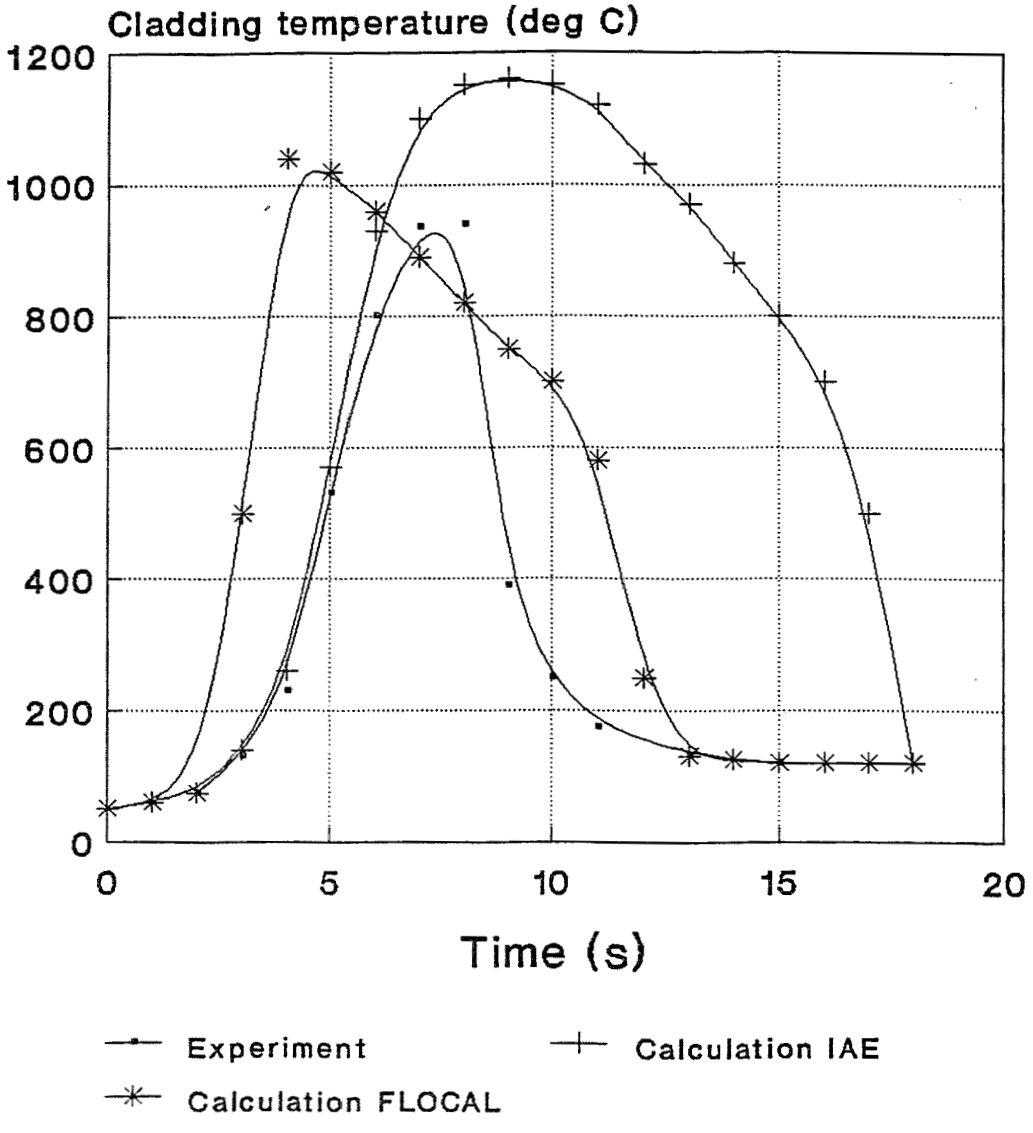

Fig.9 Results for a RIA experiment at the IGR facility , subcooling T = 80 K, E = 360 cal/g , = 300 ms